

Diagnostics of RF coupling in H-ion sources as a tool for optimizing source design and operational parameters

Stefan Briefi, D. Zielke, David Rauner, Ursel Fantz

Angaben zur Veröffentlichung / Publication details:

Briefi, Stefan, D. Zielke, David Rauner, and Ursel Fantz. 2022. "Diagnostics of RF coupling in H-ion sources as a tool for optimizing source design and operational parameters." *Review of Scientific Instruments* 93 (2): 023501. <https://doi.org/10.1063/5.0077934>.

Diagnostics of RF coupling in H^- ion sources as a tool for optimizing source design and operational parameters

Cite as: Rev. Sci. Instrum. **93**, 023501 (2022); <https://doi.org/10.1063/5.0077934>

Submitted: 08 November 2021 • Accepted: 15 January 2022 • Published Online: 01 February 2022

Published open access through an agreement with Max Planck Institute for Plasma Physics

 S. Briefi,  D. Zielke,  D. Rauner, et al.

COLLECTIONS

Paper published as part of the special topic on [Ion Source Diagnostics](#)



View Online



Export Citation



CrossMark

ARTICLES YOU MAY BE INTERESTED IN

[Emission spectroscopy of negative hydrogen ion sources: From VUV to IR](#)

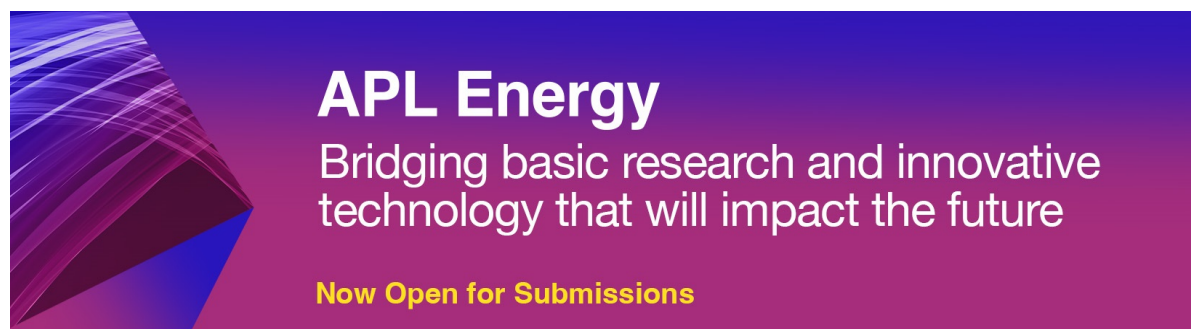
Review of Scientific Instruments **92**, 123510 (2021); <https://doi.org/10.1063/5.0075491>

[Overview of diagnostics on a small-scale RF source for fusion \(ROBIN\) and the one planned for the diagnostic beam for ITER](#)

Review of Scientific Instruments **93**, 023504 (2022); <https://doi.org/10.1063/5.0076009>

[Ion beam intensity and phase space measurement techniques for ion sources](#)

Review of Scientific Instruments **93**, 011501 (2022); <https://doi.org/10.1063/5.0075110>



APL Energy
Bridging basic research and innovative
technology that will impact the future
Now Open for Submissions

Diagnostics of RF coupling in H⁻ ion sources as a tool for optimizing source design and operational parameters

Cite as: Rev. Sci. Instrum. 93, 023501 (2022); doi: 10.1063/5.0077934

Submitted: 8 November 2021 • Accepted: 15 January 2022 •

Published Online: 1 February 2022



S. Briefi,^{1,a)} D. Zielke,¹ D. Rauner,² and U. Fantz^{1,2}

AFFILIATIONS

¹Max-Planck-Institut für Plasmaphysik, Boltzmannstr. 2, 85748 Garching, Germany

²AG Experimentelle Plasmaphysik, Universität Augsburg, 86135 Augsburg, Germany

Note: This paper is a part of the Special Topic Collection on Ion Source Diagnostics.

a) Author to whom correspondence should be addressed: stefan.briefi@ipp.mpg.de

ABSTRACT

Radio frequency (RF) driven H⁻ ion sources are operated at very high power levels of up to 100 kW in order to achieve the desired performance. For the experimental setup, these are demanding conditions possibly limiting the source reliability. Therefore, assessing the optimization potential in terms of RF power losses and the RF power transfer efficiency η to the plasma has moved to the focus of both experimental and numerical modeling investigations at particle accelerator and neutral beam heating sources for fusion plasmas. It has been demonstrated that, e.g., at typical neutral beam injection ion source setups, about half of the RF power provided by the generator is lost in the RF coil and the Faraday shield due to Joule heating or via eddy currents. In a best practice approach, it is exemplarily demonstrated at the ITER RF prototype ion source how experimental evaluation accompanied by numerical modeling of the ion source can be used to improve η . Individual optimization measures regarding the Faraday shield, the RF coil, the discharge geometry, the RF driving frequency, and the application of ferrites are discussed, which could reduce the losses by a factor of two. The provided examples are intended as exemplary guidelines, which can be applied at other setups in order to achieve with low-risk effort an optimized ion source design in terms of reduced losses and hence increased reliability.

© 2022 Author(s). All article content, except where otherwise noted, is licensed under a Creative Commons Attribution (CC BY) license (<http://creativecommons.org/licenses/by/4.0/>). <https://doi.org/10.1063/5.0077934>

I. INTRODUCTION

One of the key features of radio frequency (RF) driven H⁻ ion sources, which are realized as inductively coupled plasmas (ICPs), is their capability to operate at considerably high power levels while being considered maintenance-free. Therefore, the concept has been chosen for the neutral beam injection (NBI) systems of the fusion experiment ITER,¹ and it is often applied as the front-end particle source for accelerators,^{2–4} as both recipients require maximum reliability. However, due to the technological progression, state-of-the-art (and envisaged future) accelerator and NBI systems impose challenging requirements, which implies that RF ion sources have to operate at increasingly demanding conditions.

As an example, the ion sources for ITER NBI need to operate low pressure (0.3 Pa) hydrogen or deuterium plasmas continuously

for up to 3600 s. The discharges are generated in eight so-called drivers each having a volume of about 8 l and being powered with up to 100 kW (driving frequency 1 MHz) in order to meet the imposed requirements.¹ For accelerator sources, μ s/ms-scale pulsed operation at slightly higher hydrogen pressures in the Pa regime is required, while the typical RF power levels are still around 50 kW (driving frequency 2 MHz) despite the much smaller volume of only about 0.3 l.^{2–4}

Due to the considerable power levels required in these sources, high currents $\mathcal{O}(100\text{ A})$ and voltages $\mathcal{O}(10\text{ kV})$ are imposed on the RF system. This causes high stress on the components of the RF circuit, which is obviously critical in view of maximum source reliability. In particular, the high voltage poses the risk of arching, for example, between the RF coil windings.^{5–7} Even though the typical operating frequencies of 1 or 2 MHz are lower than, for example, the

industrial standard of 13.56 MHz effectively reducing the occurring RF voltages (but increasing the currents), the combined required operating conditions have been proven to be close to the technical and physical limits.

Against this background, assessing the RF power coupling to the plasma has recently moved to the focus of ion source characterization and understanding. In general, not all RF power provided by the generator can be utilized for the plasma heating itself, even when ideal matching conditions are achieved: inevitably, losses occur due to Joule heating in the conductors and due to induced eddy currents in metallic components. In addition, the capability of the plasma to absorb the provided power depends on multiple interlinked factors, including RF parameters, discharge conditions, presence of external magnetic fields, and source/vessel geometry. A key parameter for the characterization and quantification of these processes is the RF power transfer efficiency η , which is defined as the fraction of power actually coupled to the plasma itself in relation to the totally provided RF power.

In general, the losses occurring in RF discharges can be significant, which has been demonstrated multiple times in the past at laboratory scale plasmas.^{8–12} For RF driven H^- ion sources, η has been recently investigated at the ITER prototype source at the BATMAN Upgrade test facility¹³ and at the full-size ITER NBI ion source at the test stand SPIDER¹⁴ (whereas no comparable investigations have been carried out for particle accelerator sources to the authors' knowledge up until now). It has been shown that the measured RF power transfer efficiency is only around 50%. This observation clearly illustrates two very important aspects: First and quite generally, the RF power delivered by the generator cannot be considered as a good quantity on its own, i.e., when used to directly compare parameters and performances of different RF sources. Due to the occurring losses, the RF power actually utilized for the plasma generation, which determines the plasma parameters and their spatial profiles, may be considerably lower and is depending strongly on various operating conditions as well as the design or geometry of the individual setup. Hence, for a meaningful benchmark and comparison, the power coupled to the plasma P_{plasma} should be used, making the determination of the RF power transfer efficiency indispensable (while being comparably easy-to-measure, in fact).

Second, the observation that about half of the provided RF power cannot be utilized for the intended purpose of plasma heating clearly illustrates that there is significant room for optimization (including the demands on cooling the source components). One reason for this somewhat surprisingly large remaining potential lies most likely within the development history of RF driven ion sources, as many of their properties have been inherited from previous systems that were operated at less demanding conditions. In course of their adaption to the requirements of state-of-the-art scenarios, however, little or no target-aimed optimizations in view of an optimized RF power transfer efficiency have been conducted. In conclusion, improving η possibly allows for reducing the required RF power level considerably. This would strongly reduce the strain on the RF system increasing the source reliability while maintaining the required source performance.

In this context, the present paper aims to address and discuss the most essential aspects of RF power coupling and its diagnostics at RF driven ion sources. First, an overview of the typical setup of the RF circuit is given, followed by a brief overview of the defining

principles and physics of the RF plasma heating mechanisms at ion source relevant conditions. As it will be illustrated, the experimental methodology to determine the RF power transfer efficiency itself is indeed fairly straightforward and relatively easy-to-apply, but the interpretation and understanding of the underlying processes is complex. Hence, dedicated numerical modeling approaches are essential to appropriately assess and understand both the aspect of occurring RF losses and the mechanisms of power absorption by the plasma. Finally, by incorporating experimental data as well as modeling results, it will be illustrated how an appropriate consideration of the RF power coupling allows identifying means for target-aimed optimization of existing ion sources.

II. INDUCTIVE COUPLING IN RF ION SOURCES: FUNDAMENTALS

A. Setup of the RF circuit

RF driven ion sources are typically realized as cylindrical ICPs, where a helical multi-turn RF coil is wrapped around the dielectric plasma chamber^{2,3,15} or placed directly inside the plasma volume.^{3,4} The power is supplied by an RF generator, which can be based on amplifier tubes or solid-state technology. In between the RF generator and the coil, a matching network is installed that tunes the impedance of the entire load (plasma, RF coil, and matching network combined) to a pure real resistance of typically 50 Ω , required at the output connector of the generator. This ensures that there is no reactive power circulating in the transmission line between the RF generator and the matching network (i.e., the phase shift between RF voltage and current is minimized), which avoids strong stress on the components and ensures an optimized power transfer to the load as the generator is operated at its intended working point.

The setup of the matching network itself depends on the impedance values of the load, which is, in turn, determined by the plasma and operational parameters (such as electron density and temperature as well as the pressure and driving frequency).^{16,17} Typically, it is either realized as L-, γ -, or Π -type (see Fig. 1 for the details). Sometimes, also inductances (i.e., a coil) or even (ohmic) resistors are installed when a matching cannot be achieved only with capacitors. However, with these solutions, losses occur at the coil (resistor) in the matching network, whereas capacitors can be assumed lossless in a good approximation. Therefore, it is advisable to rather adapt the topology for achieving a proper matching than installing lossy components. It might be necessary to include the transmission line between the generator and the matching circuit in the impedance matching considerations as the line has a certain inductivity and capacitance per unit length.

It should be noted that the length of the connection between the matching network and the RF coil should be as short as possible. The conductors of this connection are often realized as bare copper tubes, so they have to be separated by several centimeters in order to avoid breakdowns. When the conductors are long, the loop between the matching network and the RF coil spans over a large area, leading to a high parasitic inductivity, causing unintended power transfer issues.

An improper matching (i.e., the impedance seen by the generator differs from a pure real 50 Ω value) effectively results in less power that is delivered to the load, sometimes given as reflected power or as a voltage standing wave ratio (VSWR) differing from

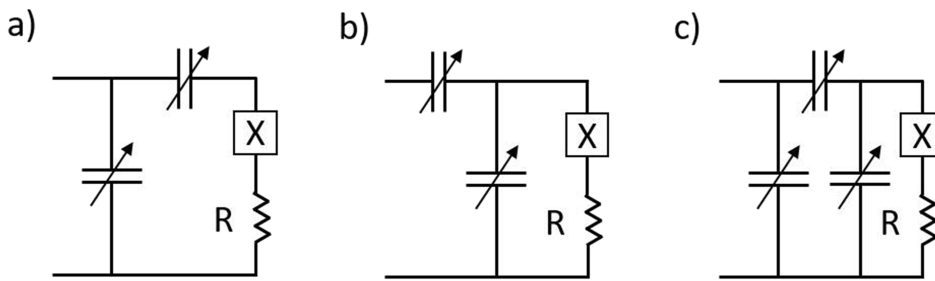


FIG. 1. Typical layouts of a matching network: (a) standard or L-type, (b) alternative or γ -type, and (c) Π -type. X and R depict the imaginary and real parts of the plasma load impedance.

unity. This results from the phase shift between the RF voltage and current, which is then existing. When a strong mismatch is present, it might be even possible that the RF generator runs toward its voltage or current limits, effectively restricting its output power. In such a condition, the amount of power that is delivered to the load is very limited. However, the load present in RF driven ion sources can usually be matched perfectly. For the rest of this paper, it is assumed that this condition is always present. It should be noted that a matching to 50 Ω can cause frequency flips in amplifier tubes, preventing a stable generator operation.¹⁸ In such cases, either an intentional mismatch is realized and/or an additional resistor is introduced at the output of the RF generator in order to achieve stable operation.^{18,19} Nevertheless, both measures lead to a reduced power available for plasma generation compared to the nominal generator power.

In some experimental setups, a high voltage insulation transformer is included in the matching network.¹⁵ This is required if the ion source itself is on the high voltage potential for the extraction of the H^- ions but the generator is on the ground potential. Typically, this transformer is equipped with ferrite cores. The exact type of the ferrite has to provide a high magnetic permittivity in order to ensure good coupling but also low losses at the required frequency. At the example of the ITER prototype source being installed at the BATMAN Upgrade testbed with a ferrite core transformer in the matching network, the additional power losses introduced by the transformer were determined as 10%–15%, i.e., η was reduced from around 50%–55% without the transformer to 35%–45% when the transformer was applied.¹³

B. ICP working principle and RF plasma heating mechanisms

In an inductively coupled plasma, the alternating current of the RF coil produces an electromagnetic field surrounding the coil. The electric component of this field forces the free electrons in the plasma to oscillate harmonically at the driving frequency. While performing these oscillations, the electrons collide with the background neutral gas and their directed kinetic energy is transformed into thermal energy. An RF current density forms in an RF skin layer of the plasma (typically in the mm-range), and the heating can be calculated as the product of the current density and the electric field. This well-known mechanism is called local (collisional) Joule heating. The electromagnetic fields and the plasma current are exponentially damped in the localized skin layer. Under typical conditions in RF ion sources, the contribution of the plasma ions to the plasma current is negligible because of the comparably larger ion

mass.¹⁶ Consequently, the plasma ions are not directly heated by the RF electric field.

At pressures below about 1 Pa, collisions between the electrons and the neutral background gas are too infrequent to explain the experimentally observed electron heating.²⁰ At low pressures, the so-called nonlocal (collisionless) heating mechanism is used to explain the power transfer to the electrons: a thermal electron is assumed to come from the bulk plasma and is reflected by the plasma sheath. If the electron travel time through the RF skin layer is short compared to the RF timescale, the electron experiences the RF electric field as almost constant. It can thus gain net momentum and energy.^{21,22}

In the typical descriptions of the local (collisional) Joule heating as well as the nonlocal (collisionless) heating, the impact of the RF magnetic field is neglected. However, the magnetic RF field in RF ion sources is typically rather large $\mathcal{O}(100\text{G})$ because of the large applied powers and the rather low frequencies, which lead to a magnetization of the electrons and to nonlinear effects, such as the ponderomotive force.²³ This has to be accounted for in a self-consistent description of the plasma heating mechanism in RF ion sources (see Sec. II E).

C. Measuring the RF power transfer efficiency

Apart from the intended power transfer to the plasma itself, ICPs are inevitably prone to power losses effectively reducing the power transmitted to the plasma compared to the total RF power supplied by the generator. Joule heating, for instance, produces energy losses in the skin depth of the copper RF coil and in the transmission lines as well as in electric connections via contact resistances. Additionally, eddy currents are driven in conductive materials, especially near the coil. These are, e.g., the metallic support structure and components, such as a Faraday shield, which is used in NBI ion sources as a dedicated measure to suppress capacitive coupling and hence protect the dielectric cylinder from plasma erosion due to a high sheath potential. All the aforementioned power losses comprise the network losses P_{net} . These are conveniently quantified by a network resistance R_{net} , i.e., $P_{\text{net}} = \frac{1}{2} R_{\text{net}} I_{\text{RF}}^2$, where I_{RF} is the RF coil current amplitude. The fraction of the power that is absorbed by the plasma is quantified by the RF power transfer efficiency η ,

$$\eta = \frac{P_{\text{plasma}}}{P_{\text{RF}}} = \frac{P_{\text{RF}} - \frac{1}{2} R_{\text{net}} I_{\text{RF}}^2}{P_{\text{RF}}}. \quad (1)$$

Herein, P_{plasma} and P_{RF} denote the power absorbed by the plasma and the RF power supplied by the generator, respectively.

From Eq. (1), η can be determined experimentally by a subtractive method.⁸ The network resistance R_{net} is quantified when there

is no plasma discharge. This is realized by suppressing ignition, in practice, either by venting the system or by suppressing gas feeding. The supplied RF power P_{RF} (which is in this case equal to P_{net}) and the coil current I_{RF} are simultaneously measured. The latter can be determined via a current transformer positioned around a feed line of the RF coil. Typically, commercially available current transformers allow for a rather precise measurement of the RF current (relative error below 5%) if read out by an oscilloscope of sufficient bandwidth. The RF power supplied by the generator is often quantified by internal directional couplers in the RF generator. However, it should be noted that the accuracy of this measurement strongly depends on the impedance of the load (i.e., the matching conditions). If the load can be matched closely to the typically required 50 Ω , the determination of the delivered RF power is precise. However, if the conditions do not allow matching the load, the accuracy of the measured RF power (forward and reflected) decreases significantly, which may non-negligibly affect the determination of η as well. A possibility to improve the measurement accuracy would be the application of dedicated external in-line voltage, current, and phase shift measurements. However, especially a precise phase shift measurement is not an easy task in the MHz-range and in addition at the required high power levels.

It is advisable to perform the measurements without plasma at sufficiently low powers to protect the network components from too high voltages that cause electric arcs and high thermal stresses. For each measured point, the matching capacities are adjusted such that perfect matching is obtained, i.e., the reflected power from the network should be as low as possible. Another convenient method to achieve perfect matching is to slightly change the applied frequency (e.g., in the range of 1% of f_{RF}) if permitted by the RF generator. This limited change in f_{RF} does almost not change the skin depth in the conductors and hence R_{net} remains substantially unchanged. The network resistance R_{net} is readily obtained from a linear fit of P_{net} over $\frac{1}{2} I_{\text{RF}}^2$ (see Fig. 2 for an exemplary fit).

After the determination of R_{net} , the RF power transfer efficiency η follows from Eq. (1) with the P_{RF} and I_{RF} values measured during plasma operation. In practice, it is advisable to perform the measurements without plasma right after the ones with plasma to ensure

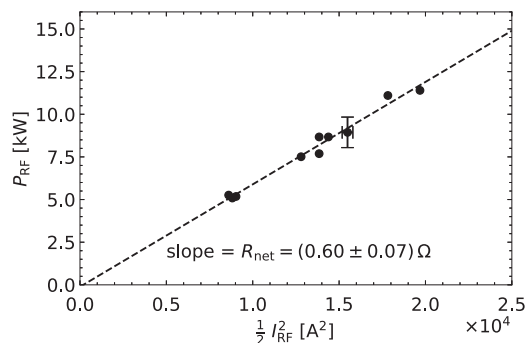


FIG. 2. The network resistance R_{net} is experimentally obtained from a linear fit of the RF power supplied by the generator P_{RF} over $\frac{1}{2} I_{\text{RF}}^2$, where I_{RF} is the RF coil current amplitude. Figure reproduced with permission from Zielke *et al.*, J. Phys. D: Appl. Phys. **54**(15), 155202 (2021). Copyright 2021 Author(s), licensed under a Creative Commons Attribution (CC BY) license.

that temperature effects on R_{net} (i.e., the conductivity of a conductor decreases with increasing temperature) are counteracted and ideally negligible.

An inherent drawback of the described method for determining η is that screening of the RF fields by the plasma cannot be taken into account, since R_{net} has to be determined without plasma. This means that it is implicitly assumed that R_{net} in plasma and R_{net} in vacuum are equal. However, when RF fields that drive eddy currents in metallic source components are shielded by the discharge itself, the loss resistance in plasma is actually lower. Therefore, the described method yields, in general, only a lower bound of η .

There are also other methods reported in the literature to determine the power transfer in RF discharges, which rely on the same or comparable fundamental assumptions yet are distinct mostly from a methodical point of view, e.g., by utilizing a network analyzer and measuring the voltage instead of current.²⁴ However, at ion sources, an application of other methods, which are not based on the above-described procedure, has not been reported up until now.

At laboratory experiments operating typically at much lower power levels compared to RF ion sources, RF power transfer efficiencies of 90% or even above can well be achieved in rare gases¹⁰ without a special effort concerning the setup design. In molecular hydrogen/deuterium discharge, however, there are more power loss channels due to the more complex plasma chemistry and higher losses to the wall because of the small particle masses compared to rare gas discharges. This leads, in general, to a lower electron density and higher electron temperature, reducing the RF power transfer efficiency. Nevertheless, also in hydrogen/deuterium laboratory discharges operated at low excitation frequency and low pressure, values of η up to 90% can be achieved.¹¹ However, the operational parameter space where these high RF power transfer efficiencies can be obtained is quite narrow and rapidly drops to values below 40% when, e.g., the pressure is varied.¹¹

As especially the pressure is a fixed operational parameter for RF driven ion sources, care has to be taken that the RF power transfer efficiency is optimized there. At the experimental setups being typical for NBI H^- ion sources, a surprisingly low η between 45% and 65% was found, depending mainly on the filling pressure.^{13,14} Therefore, it should be identified what the cause of these high losses is and ways for improving η should be pointed out.

D. Modeling RF coupling: Network losses

While the measurement of the RF power transfer efficiency is—from an experimental point of view—a rather easy-to-apply technique, its interpretation and analysis is a far more challenging task. It requires the simultaneous assessment of RF power absorption both within the network (i.e., the losses) and the plasma side. To consider both aspects appropriately, dedicated modeling approaches have to be conducted.

State-of-the-art modeling of network losses, i.e., Joule heating in the RF coil and eddy currents in components such as the Faraday shield, is based on the finite elements method (FEM).^{25,26} Here, a wave equation derived from Maxwell's equations is solved in a 3D domain V . The numerical effort is significantly reduced by assuming the time harmonic approximation, i.e., $\forall \mathbf{r} \in V : \mathbf{E}_{\text{RF}}(\mathbf{r}, t) = \text{Re}\{\tilde{\mathbf{E}}_{\text{RF}}(\mathbf{r})e^{i\omega_{\text{RF}}t}\}$ (and the same applies for \mathbf{B}_{RF}), where Re denotes the real part and $\tilde{\mathbf{E}}_{\text{RF}}$ denotes the complex electric RF field amplitude

(indicated by a tilde). In this case, the wave equation simplifies to

$$\nabla^2 \tilde{\mathbf{E}}_{\text{RF}} + \frac{\omega_{\text{RF}}^2}{c_0^2} \tilde{\epsilon}_r \tilde{\mathbf{E}}_{\text{RF}} = 0. \quad (2)$$

In this equation, the angular driving frequency is given by $\omega_{\text{RF}} = 2\pi f_{\text{RF}}$ and c_0 and $\tilde{\epsilon}_r$ denote the speed of light in vacuum and the complex relative dielectric permittivity, respectively. The latter is defined as

$$\tilde{\epsilon}_r = 1 - i \frac{\tilde{\sigma}}{\omega_{\text{RF}} \epsilon_0}. \quad (3)$$

Herein, ϵ_0 and $\tilde{\sigma}$ denote the permittivity of vacuum and the medium's conductivity, respectively. Most of the domain where the wave equation is solved is assumed to be vacuum; hence, $\tilde{\sigma}_{\text{vacuum}} = 0$ is used there. An impedance boundary condition²⁷ is applied at all conducting components to avoid resolving the small skin depth, which is around 65 μm in copper at 1 MHz. Concerning the numerical effort, the detailed complex 3D objects that are present in an RF ion source (e.g., a Faraday shield with a considerable number of thin slits with a width in the mm range¹⁵) can just barely be handled on a single workstation. Therefore, the modeling of the plasma part cannot be included in a way that the RF power absorption, plasma chemistry, and the development of spatial plasma parameter profiles are considered self-consistently within the EM model. Nevertheless, the screening effect of the plasma has still to be accounted for, although in a simplified manner. Therefore, the cold plasma approximation¹⁶ is typically applied, where the RF Lorentz force as well as electron advection and viscosity are neglected. From this follows the well-known expression for the complex valued plasma conductivity,

$$\tilde{\sigma}_{\text{plasma}} = \frac{e^2 n_e}{m_e (i\omega_{\text{RF}} + \nu_{e,n})}. \quad (4)$$

Herein, e , n_e , m_e , and $\nu_{e,n}$ denote the elementary charge, electron density, mass, and the elastic momentum transfer frequency between the electrons and the neutral particle background, respectively.

The conductivity depends on the spatial distribution of the plasma parameters n_e and $\nu_{e,n}(T_e, n_n)$, which is a function of the electron temperature T_e and the neutral gas density n_n . Either these plasma parameters are assumed uniform or their spatial profiles are used as model inputs.

The simplifying assumptions regarding the momentum balance as well as the input of plasma parameter profiles yield that the electromagnetic 3D models are not self-consistent with respect to the discharge properties. This leads to a very limited predictive capability concerning the plasma part of the power absorption. However, as the exact spatial distribution of the RF power deposition within the plasma volume has typically only little impact on the network losses, electromagnetic models are still able to calculate the complex impedance of the network components (i.e., the network resistance R_{net}) well within the experimental error bars.²⁸ It should be noted, though, that in some cases, changes in the ion source geometry (e.g., when the diameter of the discharge chamber is varied) may strongly affect the plasma parameter profiles.²⁹ It is then mandatory to perform iterative calculations of the plasma and network models in order to capture all effects consistently.

E. Modeling RF coupling: Power transfer to the plasma

A predictive description of the RF power coupling to the discharge has to account for the spatial profiles of the plasma parameters (in essence density, flux, and temperature of the plasma particles), which adjust in accordance with the spatial profiles of the electromagnetic fields. For this reason, numerically cheap global 0D models cannot be used in a self-consistent modeling approach. On the other hand, kinetic models, such as particle-in-cell simulations, are numerically too expensive for the larger plasma volumes and densities in typical RF ion source discharges.

Situated in between the two above approaches in terms of physical viability and numerical cost are the fluid models, which are commonly used to describe the RF power coupling, however, currently only in 2D simulation domains^{30–32} due to the still considerable numerical effort. Here, particle-, momentum-, and energy-transport equations are solved in time and space for the neutral hydrogen atoms and molecules as well as for the charged ions H^+ , H_2^+ , and H_3^+ and for the electrons. For the self-consistent calculation of the plasma potential, Poisson's equation is solved. The magnetic and electric RF fields are calculated from Ampère's and Faraday's law, respectively. Carefully compiled sets of collision cross sections are used to quantitatively account for the various elastic and inelastic collisions between the different particle species.^{33–35} Inputs of a self-consistent model are the coil and discharge geometry, the RF power supplied from the generator P_{RF} , the driving frequency f_{RF} , the network resistance R_{net} , and the influx of hydrogen molecules as well as the gas conductance of the extraction grid system. These parameters are all specified by the experimental setup, although for R_{net} only in an indirect way, so it can either be determined experimentally (as described in Sec. II C) or modeled (see Sec. II D). More details on setting up a self-consistent fluid model to describe RF ion source discharges can be found in Ref. 29; a short overview is given here.

In order to describe the power coupling between the RF fields and the plasma electrons in a self-consistent way, the following points are considered: (i) The plasma current density is provided as the right-hand side of Ampère's law. (ii) In the electron energy transport equation, the product of the plasma current density and the electric RF field provides the inductive input power per unit volume. (iii) In the electron momentum transport equation, different forces (RF electric force, RF Lorentz force, and friction force) acting on the electrons are accounted for. Typically, RF ion source discharges are in the nonlinear or in the local skin effect regime at large magnetic RF fields. Figure 3 exemplarily shows the operational range of the ITER prototype source.

Because of the large magnetic RF field in this regime, it is important to retain the nonlinear RF Lorentz force in the electron momentum transport equation.^{23,30,32} Theoretical modeling^{36–39} and experimental measurements of the plasma density¹³ indicate that the RF Lorentz force compresses the plasma via the ponderomotive effect. However, when the RF Lorentz force is accounted for in the electron momentum transport equation, the compression effect is largely overestimated, wherefore no numerical steady state solution was found.³⁰ To resolve this issue it was recently proposed to include the local collisional expression for the viscosity of the electrons in the electron momentum transport equation. By doing so, the RF current density diffuses deeper into the plasma and its absolute value is thus decreased, which reduces the impact

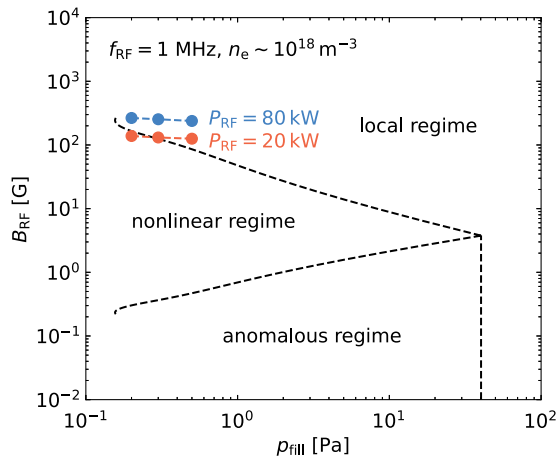


FIG. 3. Regions of anomalous, nonlinear, and local RF skin effect regime (see Ref. 32 for a detailed explanation of the different regimes) at a fixed driving frequency $f_{RF} = 1$ MHz for various filling pressures p_{fill} and magnetic RF field strengths B_{RF} . The RF ion source operates mostly in the high magnetic RF field region of the local regime. Figure adapted with permission from Zielke *et al.*, Plasma Sources Sci. Technol. **30**, 065011D (2021). Copyright 2021 Author(s), licensed under a Creative Commons Attribution (CC BY) license.

of the ponderomotive effect.²⁹ Note that this approach is consistent with the local skin effect regime, where the RF ion sources mostly operate. Beyond that, a description of the particle, momentum, and energy transport equations for the neutral species (in contrast to simply assuming a uniform neutral background, as is often done in plasma fluid models) is mandatory to capture neutral depletion via ionization,⁴⁰ which is especially pronounced at high power levels.²⁹

When the appropriate terms in the electron momentum transport equation (to account for the RF Lorentz force and for diffusion of the RF current) as well as a description of the neutrals (to account for neutral depletion) are used, RF coil currents and plasma parameter profiles that scale as in the experiment are obtained from the model. Even absolute agreement between the modeled and measured quantities seems to be within reach when intrinsic 3D effects,

such as the magnetic drift of the plasma due to the highly non-uniform magnetic fields present in the ion sources, are taken into account.²⁹ Concerning the numerical effort, 2D fluid models have a typical run-time in the order of a few hours on a common workstation. Extending the simulation domain to 3D is what should be the next logical step. The strongly increased numerical effort for solving the model requires the usage of a computational cluster.

III. OPTIMIZING RF POWER COUPLING

From Eq. (1), optimizing the RF power coupling can be thought of as a twofold process: reducing the losses in the RF network and/or increasing the plasma's capability to absorb power. However, these points can only be considered separately in certain cases as typically ion source setup changes affect both the network losses and the plasma properties.

When one aims at reducing the network losses, an identification of those components where significant power is deposited has to be carried out first. This task can be achieved via electromagnetic models as described in Sec. II D. Such an investigation has recently been carried out for the ITER prototype ion source.²⁸ For this setup, 76% of the losses occurred due to eddy currents in the Faraday shield and 20% are caused due to Joule heating of the coil. The remaining few percent could be assigned to eddy-current induced losses in metallic source components. Figure 4 shows a color plot of the power loss density obtained from the 3D EM model where the spatial distribution can be seen. The numerical results of R_{net} have successfully been benchmarked against the experimentally obtained network resistance.^{13,28}

The distribution of the losses depends strongly on the specific setup. In the design of H^- sources for particle accelerators, a Faraday shield is typically not included. First, the presence of capacitive coupling helps igniting the plasma at the required repetition rate, which is often an issue. Second, due to the very low integrated plasma-on-time, the dielectric wall material does not suffer significantly from chemical sputtering. The omission of the Faraday shield should be beneficial concerning the network losses. However, absolute numbers require dedicated experimental or numerical investigations, which are not available for accelerator ion sources up until now.

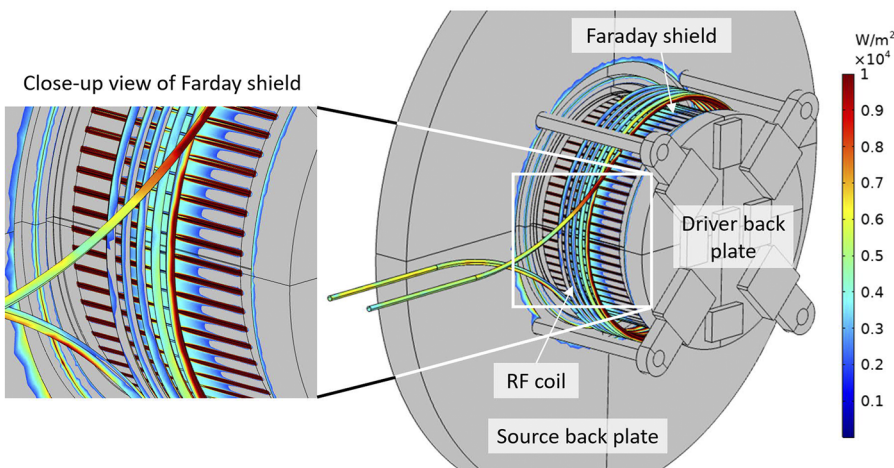


FIG. 4. Color plot of the power loss density calculated with a 3D resolved EM model of the ITER reference source setup.⁴¹

At some NBI ion source test stands, the whole driver setup is put in a vacuum chamber in order to reduce the probability of arcing between the coil windings. If the distance between the RF coil and the metallic wall of this chamber is not very large, significant power losses due eddy currents might occur in the wall of the vacuum chamber.⁴²

In the following, possibilities for improving the RF power transfer efficiency are discussed for the most part at the example of the ITER prototype ion source, as only for this setup a systematic investigation of both the network losses and the power transfer to the plasma is available.

A. Faraday shield

As the highest part of the losses present in the ITER reference ion source is caused by the Faraday shield, its optimization is addressed first. In doing so, it is mandatory to consider both the network resistance as well as the RF-to-plasma coupling. However, a simplified treatment of the plasma as described in Sec. II D is sufficient for this purpose, as the plasma properties, such as the spatial particle distributions, are not altered significantly as long as the volume to surface ratio of the plasma does not change.

Regarding R_{net} , its value increases with the slit number and slit length, as the loss area for eddy currents is increased.²⁸ This somewhat counter-intuitive result would therefore suggest that for reducing the network losses, one should make the Faraday shield as opaque as possible for the RF fields (i.e., less and smaller slits).

However, this is obviously not beneficial for sustaining the discharge in the first place, as for the best RF-to-plasma coupling, the Faraday shield should be as transparent as possible. This is also reflected by the EM model when the RF power absorption by the plasma is considered: despite the higher network resistance, increasing the slit number, the slit length, and the slit width is beneficial for the RF power transfer efficiency, as the positive impact of the better coupling between the RF fields and the plasma prevails the negative influence of the higher R_{net} .²⁸

Concerning the thickness of the Faraday shield (or, in general, the distance between the RF coil and the plasma), both the R_{net} optimization and the RF-plasma coupling yield the best results when the thickness is as low as possible.^{28,42}

For the design optimization of the Faraday shield, some boundary conditions have to be considered. First, it has to screen the radial electric RF field component between the coil and the plasma, preventing a large slit width. Second, when the ion source is operated in the CW mode, water-cooling channels need to be incorporated in the metallic legs between the slits. This leads to a minimum thickness of about 3 mm and a minimum distance of about 5 mm between the slits. For the ITER reference source, the slit number can still be increased from 75 to 119.⁴¹ According to the EM model, this slightly increases the network resistance by around 5%, but due to the better power coupling between the RF fields and the plasma, the RF power transfer efficiency increases from around 45%–55%.

B. RF coil

For the losses caused by the RF coil itself, the EM model indicates that it is beneficial to increase the number of coil windings, with the boundary condition of keeping a certain distance between

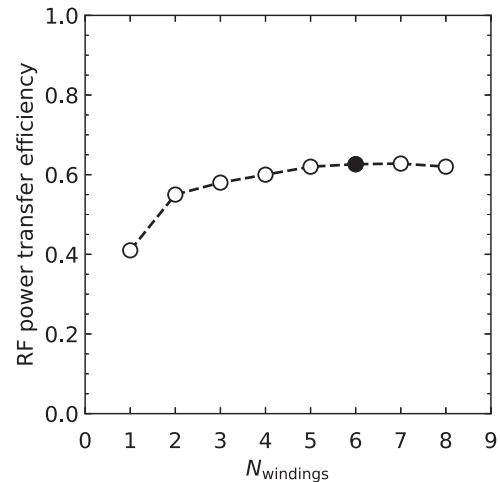


FIG. 5. RF power transfer efficiency as a function of the number of coil windings N_{windings} , calculated using the electromagnetic model together with the self-consistent RF power coupling model (the current winding number of six is marked with a full symbol). Figure adapted with permission from D. Zielke, "Development of a predictive self-consistent fluid model for optimizing inductive RF coupling of powerful negative hydrogen ion sources," Ph.D. thesis, University of Augsburg, 2021.²⁹

the coil windings and toward conducting components surrounding the RF coil, i.e., the driver and source back plates.⁴¹ Other coil parameters, such as the coil wire diameter and coil spread, do not significantly reduce the network losses. However, changing the coil directly affects the distribution of the RF fields inside the plasma chamber, most likely affecting the power absorption within the plasma. In order to investigate the mutual effect, a self-consistent plasma model (see Sec. II E) has to be applied.

The network resistance obtained from the 3D EM model for the different number of coil windings is used as input for the fluid plasma model calculating the power absorbed by the discharge in each case. Figure 5 shows the obtained RF power transfer efficiency, which increases up to a winding number N_{windings} of three but saturates for a larger N_{windings} . This saturation is a consequence from an almost constant loss power $P_{\text{net}} = \frac{1}{2} R_{\text{net}} I_{\text{RF}}^2$, where the increasing network resistance²⁸ is almost fully compensated by the decreasing coil current, which adapts due to the increasing RF coil inductance with larger N_{windings} .

C. Driver geometry

Other design optimization parameters that have an impact both on the network losses and on the plasma side are the axial driver length L_{driver} and radius R_{driver} . As shown in Ref. 29, the network resistance remains almost constant in the former case, whereas it linearly increases in the latter case due to the longer RF coil and larger Faraday shield surface. Both the larger driver length and radius increase the plasma volume and hence the region where the power coupling takes place. In the former case, this yields a considerable increase in the RF power transfer efficiency from around 60%–85%, as depicted in Fig. 6 (left). In the latter case however, the effect is superimposed by an increasing ponderomotive force, which tends to

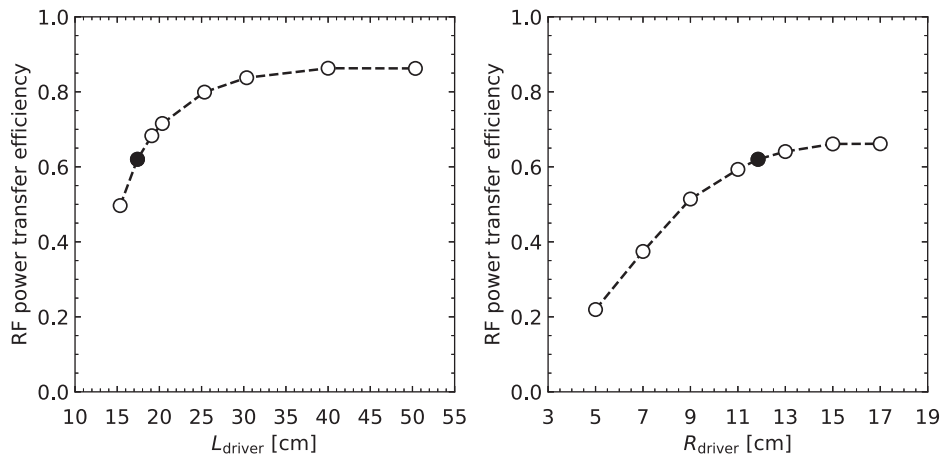


FIG. 6. RF power transfer efficiency as a function of the axial driver length L_{driver} (left) and driver radius R_{driver} (right). The full symbols indicate the values of the current (non-optimized) experimental setup. Figure adapted with permission from D. Zielke, “Development of a predictive self-consistent fluid model for optimizing inductive RF coupling of powerful negative hydrogen ion sources,” Ph.D. thesis, University of Augsburg, 2021.²⁹

push the electrons away from the RF coil and out of the RF-power-coupling region for discharges with a larger radius. Hence, the RF power transfer efficiency hardly increases when R_{driver} is increased beyond its current value of around 12 cm.

D. Driving frequency

Another important optimization parameter is the driving frequency f_{RF} . It can be shown by simple analytic theory that the network resistance scales as $f_{\text{RF}}^{1/2}$, i.e., it increases with increasing frequency due to the reduced skin depth where the RF current is driven. However, calculations show that the RF coil current amplitude for sustaining discharges with a fixed absorbed plasma power decreases considerably at larger frequencies. Hence, the RF power transfer efficiency increases from around 60% to almost 95% when f_{RF} is increased from 1 MHz to the industry standard frequency of 27.12 MHz.²⁹ Note, however, that the decreasing coil current amplitude is accompanied by an increasing coil voltage, which is not

always desirable in terms of high voltage holding of the various components. Therefore, for the ITER prototype ion source, the optimum driving frequency would be around 2 MHz, providing a significantly enhanced value of η but an almost similar RF coil voltage.²⁹

E. External magnetostatic fields

In the typical setup, magnetostatic fields are present in the form of cusp and filter fields. These fields can affect the coupling between the RF and the plasma, especially when they have non-negligible field strengths in the vicinity of the RF heating region. PIC modeling investigations at the CERN’s Linac4 ion source⁴³ revealed that the cusp magnets, which are intended to reduce plasma losses to the wall of the discharge chamber, also keep the electrons away from the heating region having a strong negative impact on the RF–plasma coupling. Experimental investigations revealed that omitting the magnetostatic cusp fields halved the RF power required for achieving similar plasma parameters.⁴⁴ A comparable impact of cusp magnets

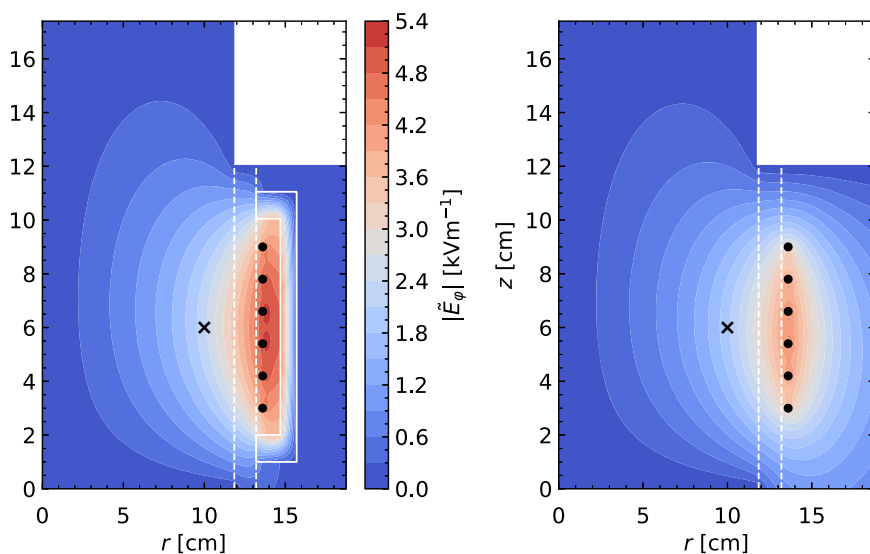


FIG. 7. Self-consistent electric field amplitude $|\vec{E}_\phi|$ calculated for a fixed filling pressure of 0.3 Pa and generator power $P_{\text{RF}} = 75$ kW for the ITER reference source setup. Left: ferrites surrounding the RF coil as indicated ($\mu_r \approx 1000$). Right: situation without ferrites for comparison. The field amplitudes at the position of the exemplary cross are $|\vec{E}_\phi| \approx 2.32$ kV with ferrites and $|\vec{E}_\phi| \approx 1.94$ kV without them.

installed in the back plate of the driver resulted from first investigations with the self-consistent fluid code applied for the ITER reference ion source.²⁹

F. Application of ferrites

Inserting ferrites in between the coil and a nearby metallic wall can strongly reduce the associated losses induced by eddy currents,⁴² as the RF fields are guided within the ferrite material effectively shielding the wall. In addition, a concentration of the RF fields within the ferrite leads, in general, to stronger fields also in the plasma chamber, as exemplarily shown for the ITER prototype ion source in Fig. 7. Here, the simulation predicts that the RF power transfer efficiency is increased from around 60% to almost 80% simply due to the changed RF field topology. However, this calculation does not account for hysteresis losses in the ferrite, which might be significant in effectively reducing η again.

Ferrites have also been applied some time ago on the ITER reference source with the aim of enhancing the RF power transfer efficiency,⁴⁵ unfortunately, without measuring η . Instead, the emission of the Balmer- α line emerging from the driver was taken as a figure of merit where no significant change could be detected when adding the ferrites to the setup. An estimation of the hysteresis losses yielded that several kW of RF power were deposited in the ferrites. This led to a quick heat-up of the material, possibly even above the Curie temperature (which was only around 125 °C) nullifying their beneficial properties. Inspection of the ferrites after the test showed that some of them also cracked. Nevertheless, the application of a different low-loss ferrite material with a high Curie temperature should be investigated together with a direct measurement of η .

IV. CONCLUSION

Experimental diagnostics of the RF power transfer efficiency η of RF driven ion sources in combination with its dedicated numerical assessment can be a powerful tool for source characterization. It provides means to elucidate a variety of practical possibilities for a significant optimization of currently operated and future RF sources in terms of RF coupling. This directly leads toward a potential reduction of the totally required RF power—a highly beneficial goal in terms of an increased source reliability.

Considering presently operated state-of-the-art RF driven NBI ion sources, about half of the power provided by the generator is not coupled to the plasma. The losses are predominantly caused by eddy currents in the Faraday shield, which is required for preventing capacitive coupling between the RF coil and the plasma. When a transformer is present in the RF circuit, the hysteresis losses within its ferrites reduce the RF power transfer efficiency by 15%. Dedicated investigations on optimizing the present source setup revealed that the following measures provide a significant enhancement of η : a more transparent Faraday screen (i.e., increasing the slit number and slit length), an increased driver length, as well as the change in the driving frequency from 1 to 2 MHz. If these measures would be combined, the RF power transfer efficiency increases to above 90% (without RF transformer), effectively reducing the losses by a factor of two.

For accelerator sources, dedicated investigations with both an EM model and a self-consistent plasma fluid model have not been

carried out up until now but should be pursued as well. Since these sources are typically not equipped with a Faraday shield, the network resistance should be considerably decreased compared to NBI ion sources, yet the RF coil is usually very close to metallic support structures. Therefore, eddy currents in these components might then be the limiting factor of the RF power transfer efficiency. Assessing the power losses in these sources can relax the water cooling requirements being especially relevant when the source is operated at a high duty factor. Optimizing the coupling between the RF fields and the plasma may furthermore ease the plasma ignition, which is often a crucial issue.

In general, the RF power transfer efficiency can be determined experimentally with rather low effort and directly reveals the optimization potential available at this specific source setup. This provides a low-risk investment with possible high gain concerning the source reliability, wherefore the investigation is highly recommended for any RF driven ion source.

ACKNOWLEDGMENTS

This work has been carried out within the framework of the EUROfusion Consortium and has received funding from the Euratom Research and Training Programme 2014-2018 and 2019-2020 under Grant Agreement No. 633053. The views and opinions expressed herein do not necessarily reflect those of the European Commission.

AUTHOR DECLARATIONS

Conflict of Interest

The authors have no conflicts to disclose.

DATA AVAILABILITY

The data that support the findings of this study are available from the corresponding author upon reasonable request.

REFERENCES

- ¹R. S. Hemsworth *et al.*, "Overview of the design of the ITER heating neutral beam injectors," *New J. Phys.* **19**(2), 025005 (2017).
- ²J. Lettry *et al.*, "Linac4 H[−] ion sources," *Rev. Sci. Instrum.* **87**(2), 02B139 (2016).
- ³R. F. Welton, M. P. Stockli, B. X. Han, S. N. Murray, T. R. Pennisi, C. Stinson, A. Aleksandrov, C. Pillar, Y. Kang, and O. Tarvainen, "H[−] ion source research and development at the Oak Ridge National Laboratory," *AIP Conf. Proc.* **2373**(1), 070004 (2021).
- ⁴A. Ueno, K. Ohkoshi, K. Ikegami, A. Takagi, K. Shinto, and H. Oguri, "110 mA operation of J-PARC cesiated RF-driven H[−] ion source," *AIP Conf. Proc.* **2373**(1), 040002 (2021).
- ⁵S. Mattei, K. Nishida, M. Onai, J. Lettry, M. Q. Tran, and A. Hatayama, "Numerical simulation of the RF plasma discharge in the Linac4 H[−] ion source," *AIP Conf. Proc.* **1869**(1), 030018 (2017).
- ⁶W. Kraus, D. Wunderlich, U. Fantz, B. Heinemann, F. Bonomo, and R. Riedl, "Deuterium results at the negative ion source test facility ELISE," *Rev. Sci. Instrum.* **89**(5), 052102 (2018).
- ⁷M. Recchia, A. Maistrello, M. Bigi, D. Marcuzzi, and E. Gaio, "Studies on the voltage hold off of the SPIDER driver coil at high radio frequency power," *AIP Conf. Proc.* **2052**(1), 040010 (2018).
- ⁸J. Hopwood, "Planar RF induction plasma coupling efficiency," *Plasma Sources Sci. Technol.* **3**(4), 460 (1994).

- ⁹V. A. Godyak, R. B. Piejak, and B. M. Alexandrovich, "Experimental setup and electrical characteristics of an inductively coupled plasma," *J. Appl. Phys.* **85**(2), 703–712 (1999).
- ¹⁰E. A. Kralkina, A. A. Rukhadze, V. B. Pavlov, K. V. Vavilin, P. A. Nekliudova, A. K. Petrov, and A. F. Alexandrov, "RF power absorption by plasma of a low-pressure inductive discharge," *Plasma Sources Sci. Technol.* **25**(1), 015016 (2016).
- ¹¹D. Rauner, S. Briefi, and U. Fantz, "RF power transfer efficiency of inductively coupled low pressure H₂ and D₂ discharges," *Plasma Sources Sci. Technol.* **26**(9), 095004 (2017).
- ¹²D. Rauner, S. Briefi, and U. Fantz, "Influence of the excitation frequency on the RF power transfer efficiency of low pressure hydrogen ICPs," *Plasma Sources Sci. Technol.* **28**(9), 095011 (2019).
- ¹³D. Zielke, S. Briefi, and U. Fantz, "RF power transfer efficiency and plasma parameters of low pressure high power ICPs," *J. Phys. D: Appl. Phys.* **54**(15), 155202 (2021).
- ¹⁴P. Jain, M. Recchia, A. Maistrello, and E. Gaio, "Experimental investigation of RF driver equivalent impedance in the inductively coupled SPIDER ion source," in International Conference on Ion Sources (ICIS2021), Canada, Vancouver, 2021.
- ¹⁵B. Heinemann, U. Fantz, W. Kraus, L. Schiesko, C. Wimmer, D. Wunderlich, F. Bonomo, M. Fröschle, R. Nocentini, and R. Riedl, "Towards large and powerful radio frequency driven negative ion sources for fusion," *New J. Phys.* **19**(1), 015001 (2017).
- ¹⁶M. A. Lieberman and A. J. Lichtenberg, *Principles of Plasma Discharges and Materials Processing*, 2nd ed. (John Wiley & Sons, Inc., Hoboken, NJ, 2005).
- ¹⁷P. Chabert and N. Braithwaite, *Physics of Radio-Frequency Plasmas*, 1st ed. (Cambridge University Press, 2011).
- ¹⁸W. Kraus, U. Fantz, B. Heinemann, and P. Franzen, "Solid state generator for powerful radio frequency ion sources in neutral beam injection systems," *Fusion Eng. Des.* **91**, 16–20 (2015).
- ¹⁹F. Gasparini, M. Recchia, M. Bigi, T. Patton, A. Zamengo, and E. Gaio, "Investigation on stable operational regions for SPIDER RF oscillators," *Fusion Eng. Des.* **146**, 2172–2175 (2019), part of the Special Issue: SI: SOFT-30.
- ²⁰V. Godyak, "Plasma phenomena in inductive discharges," *Plasma Phys. Controlled Fusion* **45**(12A), A399–A424 (2003).
- ²¹V. Vahedi, M. A. Lieberman, G. DiPeso, T. D. Rognlien, and D. Hewett, "Analytic model of power deposition in inductively coupled plasma sources," *J. Appl. Phys.* **78**, 1446–1458 (1995).
- ²²M. M. Turner, "Collisionless heating in radio-frequency discharges: A review," *J. Phys. D: Appl. Phys.* **42**(19), 194008 (2009).
- ²³V. I. Kolobov and V. A. Godyak, "Inductively coupled plasmas at low driving frequencies," *Plasma Sources Sci. Technol.* **26**(7), 075013 (2017).
- ²⁴V. A. Godyak and R. B. Piejak, "In situ simultaneous radio frequency discharge power measurements," *J. Vac. Sci. Technol. A* **8**(5), 3833–3837 (1990).
- ²⁵See www.ansys.com/products/electronics/ansys-hfss for information about the Ansys HFSS module; accessed on 13 July 2021.
- ²⁶See www.comsol.de/acdc-module for information on the COMSOL AC/DC module; accessed on 13 July 2021.
- ²⁷T. B. A. Senior, "Impedance boundary conditions for imperfectly conducting surfaces," *Appl. Sci. Res., Sect. B* **8**(1), 418 (1960).
- ²⁸S. Briefi, D. Zielke, R. Sperber, and U. Fantz, "Determining RF network losses at the H[−] ion source testbed BATMAN Upgrade via 3D electromagnetic modelling" (unpublished) (2021).
- ²⁹D. Zielke, "Development of a predictive self-consistent fluid model for optimizing inductive RF coupling of powerful negative hydrogen ion sources," Ph.D. thesis, University of Augsburg, 2021.
- ³⁰G. J. M. Hagelaar *et al.*, "Model of an inductively coupled negative ion source: I. General model description," *Plasma Sources Sci. Technol.* **20**(1), 015001 (2011).
- ³¹S. Lishev, L. Schiesko, D. Wunderlich, C. Wimmer, and U. Fantz, "Fluid-model analysis on discharge structuring in the RF-driven prototype ion-source for ITER NBI," *Plasma Sources Sci. Technol.* **27**(12), 125008 (2018).
- ³²D. Zielke, D. Rauner, S. Briefi, S. Lishev, and U. Fantz, "Self-consistent fluid model for simulating power coupling in hydrogen ICPs at 1 MHz including the nonlinear RF Lorentz force," *Plasma Sources Sci. Technol.* **30**(6), 065011 (2021).
- ³³J. P. Boeuf, G. J. M. Hagelaar, P. Sarraillh, G. Fubiani, and N. Kohen, "Model of an inductively coupled negative ion source: II. Application to an ITER type source," *Plasma Sources Sci. Technol.* **20**(1), 015002 (2011).
- ³⁴M. Bacal, "Physics aspects of negative ion sources," *Nucl. Fusion* **46**(6), S250–S259 (2006).
- ³⁵R. K. Janev, D. Reiter, and U. Samm, *Collision Processes in Low-Temperature Hydrogen Plasmas*, Berichte des Forschungszentrums Jülich Vol. 4105 (Forschungszentrum, Zentralbibliothek, Jülich, 2003), record converted from VDB: 12.11.2012.
- ³⁶V. Godyak, R. Piejak, B. Alexandrovich, and A. Smolyakov, "Observation of the ponderomotive effect in an inductive plasma," *Plasma Sources Sci. Technol.* **10**(3), 459–462 (2001).
- ³⁷A. I. Smolyakov, V. Godyak, and Y. Tyshetskiy, "Effect of the electron thermal motion on the ponderomotive force in inductive plasma," *Phys. Plasmas* **8**(9), 3857–3860 (2001).
- ³⁸D. Y. Sydorenko, A. I. Smolyakov, Y. O. Tyshetskiy, and V. A. Godyak, "Simulations of ponderomotive effects in inductively coupled plasmas," *Phys. Plasmas* **12**(3), 033503 (2005).
- ³⁹G. DiPeso, T. D. Rognlien, V. Vahedi, and D. W. Hewett, "Equilibrium profiles for RF-plasma sources with ponderomotive forces," *IEEE Trans. Plasma Sci.* **23**(4), 550–557 (1995).
- ⁴⁰A. Fruchtman, "Neutral gas depletion in low temperature plasma," *J. Phys. D: Appl. Phys.* **50**(47), 473002 (2017).
- ⁴¹S. Briefi, D. Zielke, and U. Fantz, "Inductive coupling between RF and plasma: Insights and consequences for H[−] ion sources," in International Conference on Ion Sources (ICIS2021), Vancouver, Canada, 2021.
- ⁴²P. Zhao, D. Chen, D. Li, C. Zuo, X. Li, and M. Fan, "RF simulation and improvements of an ion source test facility at HUST," *Fusion Eng. Des.* **132**, 29–36 (2018).
- ⁴³S. Mattei, K. Nishida, S. Mochizuki, A. Grudiev, J. Lettry, M. Q. Tran, and A. Hatayama, "Kinetic simulations and photometry measurements of the E-H transition in cylindrical inductively coupled plasmas," *Plasma Sources Sci. Technol.* **25**(6), 065001 (2016).
- ⁴⁴S. Briefi, S. Mattei, J. Lettry, and U. Fantz, "Influence of the cusp field on the plasma parameters of the Linac4 H[−] ion source," *AIP Conf. Proc.* **1869**(1), 030016 (2017).
- ⁴⁵W. Kraus, private communication (2021).